Realization of Universal Ion Trap Quantum Computation with Decoherence Free Qubits

T. Monz,[1] K. Kim,[1,*] A. S. Villar,[1,2,†] P. Schindler,[1] M. Chwalla,[1] M. Riebe,[1]
C. F. Roos,[2] H. Häffner,[2,‡] W. Hänsel,[1] M. Hennrich,[1] and R. Blatt[1,2]

[1]*Institut für Experimentalphysik, Universität Innsbruck, Technikerstr. 25, A-6020 Innsbruck, Austria*
[2]*Institut für Quantenoptik und Quanteninformation, Österreichische Akademie der Wissenschaften, Otto-Hittmair-Platz 1, A-6020 Innsbruck, Austria*

(Dated: September 21, 2009)

Any residual coupling of a quantum computer to the environment results in computational errors. Encoding quantum information in a so-called decoherence-free subspace provides means to avoid these errors. Despite tremendous progress in employing this technique to extend memory storage times by orders of magnitude, computation within such subspaces has been scarce. Here, we demonstrate the realization of a universal set of quantum gates acting on decoherence-free ion qubits. We combine these gates to realize the first controlled-NOT gate within a decoherence-free, scalable quantum computer.

PACS numbers: 03.67.Lx, 37.10.Ty, 32.80.Qk

Decoherence of quantum information can never be completely avoided even with perfect experimental control. It arises from the coupling of the quantum system to its environment and eventually limits the achievable precision of quantum information processing. One method to tackle faulty information storage is quantum error correction[1, 2, 3]. This approach relies on high-fidelity gates for detecting as well as correcting errors. Another strategy is to passively protect quantum information by storing the information in a decoherence-free subspace (DFS)[4]. This method has been implemented using photons[5, 6], nuclear magnetic resonance (NMR) systems[7], and trapped ions[8, 9, 10]. DFS-encoding has given rise to an impressive increase in coherence time of more than a factor of one hundred [8]. However, the use of DFSs for quantum computational operations so far was restricted to a single implementation in NMR[11]. The main challenge is to find methods to implement a universal set of gates within DFS for a given physical setup and to have sufficient experimental control to perform these gates with high fidelity.

Typically, ion trap quantum computers rely on quantum bits encoded in long lived electronic states of individual ions. Nevertheless, the phase of the qubits can deteriorate quickly which leads to a loss of encoded information. This dephasing is caused by random fluctuations of the energy difference between the qubit states $|0\rangle$ and $|1\rangle$. For qubits based on optical transitions in atoms, this decoherence mechanism is mainly caused by magnetic field noise and frequency fluctuations of the laser driving the qubit transition. In addition, for upcoming realizations of a scalable quantum computer based on segmented ion traps, ions are moved across sizable distances where magnetic field gradients lead to an additional, uncontrolled phase evolution [12]. All these types of dephasing can be overcome by encoding information in a logical qubit, realized by two physical qubits of the form $|0\rangle_L = |1\rangle_P \otimes |0\rangle_P \equiv |10\rangle_P$ and $|1\rangle_L = |0\rangle_P \otimes |1\rangle_P \equiv |01\rangle_P$ where the indices P and L denote the physical and logical basis, respectively. Ideally, the energy difference between two logical states vanishes and energy shifts common to both physical qubits do not affect the energy difference of the logical eigenstates. Thus the phase between the two logical qubits is preserved and the logical eigenstates represent a DFS with respect to the collective decoherence mechanisms described above.

In this letter, we use this encoding to implement a universal set of logical gates in a scalable quantum computer. The set is composed of single-qubit rotations and a two-qubit phase gate acting directly on the logical qubits. Sequences of such logical gates allow implementation of arbitrary quantum circuits[13, 14]. As an example, we implement the entangling controlled-NOT (CNOT) gate operation for logical qubits. We then use the CNOT gate operation, supplemented with a logical single qubit gate operation, to create Bell states in the logical subspace. Additionally, we characterize the CNOT gate operation via quantum process tomography.

Our experimental system consists of a string of $^{40}Ca^+$ ions trapped in a linear Paul trap. The physical qubits are represented by the two electronic states $S_{1/2}(m = -1/2) \equiv |S\rangle \equiv |1\rangle_P$ and $D_{5/2}(m = -1/2) \equiv |D\rangle \equiv |0\rangle_P$. Individual ion qubits, or alternatively pairs of ions, are manipulated by a focused laser beam at 729 nm, exciting the quadrupole transition between the two states $S_{1/2}$ and $D_{5/2}$ (see Fig. 1). Optical pumping initializes all ion qubits in the $|S\rangle$ state, while Doppler cooling and subsequent sideband cooling prepares the ion string in the motional ground state of the axial center-of-mass mode. An additional bit flip on one of the ions initializes the logical qubits in $|0\rangle_L = |10\rangle_P$ or $|1\rangle_L = |01\rangle_P$. Final state detection is performed using electron shelving of all ions on the $S_{1/2} \leftrightarrow P_{1/2}$ transition by detecting the ions' resonance fluorescence with a CCD camera. Absence or presence

of light corresponds to a projective measurement in the physical qubit basis $|1\rangle_P$ and $|0\rangle_P$, respectively. Details of the setup can be found in Ref. [15].

The presented work is largely based on the subsequent application of two different bichromatic gates, the conditional phase (CP) gate[16] and the Mølmer and Sørensen (MS) gate[17]. For both gates, the qubit-qubit interaction is mediated by coupling the ions to a motional mode of the ion string. The gate mechanism can be described by an off-resonantly driven quantum harmonic oscillator with a state-dependent driving force [18], i. e. a Hamiltonian $H \propto (a\exp(i\delta t) + a^\dagger \exp(-i\delta t))S_i$ where $a^\dagger$ and a represent creation and annihilation operators for motional quanta, and δ defines the detuning from the motional sideband. For the conditional phase gate, the coupling is given by $S_i = \sigma_z^{(1)} + \sigma_z^{(2)}$, whereas in the case of the Mølmer and Sørensen gate $S_i = \sigma_x^{(1)} + \sigma_x^{(2)}$. After an interaction time $\tau = 2\pi/\delta$, the harmonic oscillator returns to its initial state so that the gate acts only on the internal states of the ions. The gate action can be described as if induced by an effective Hamiltonian $H_{\text{eff}} \propto S_i^2$ that is nonlinear in the spin operators. In the following, we present how to rewrite these gates in the basis of logical qubits, thus representing building blocks for encoded quantum information.

A universal set of gate operations can be realized with arbitrary single qubit rotations in conjunction with a universal two qubit gate. In the following we will discuss our experimental realization of such a set of operations in a DFS as proposed in [19]. First, we consider arbitrary operations on a single logical qubit. We use rotations around the z-axis (σ_L^z) and the x-axis (σ_L^x) of the logical qubit's Bloch sphere. The z-rotation is implemented by addressing a single physical qubit with a laser beam far detuned from resonance that shifts the qubits energy levels due to the AC-Stark effect (see Fig. 1). Because of the identity $1_P \otimes \sigma_P^z \equiv \sigma_L^z$, the z-rotation of one physical qubit directly translates into a z-rotation on the logical qubit. Rotations by an arbitrary angle $Z(\theta) \equiv \exp(-i\ \theta/2\ \sigma_L^z)$ are controlled by the intensity and pulse length of the laser pulse. Fidelities of 98(1)% were measured for the σ_L^z gate using Ramsey experiments.

The second single logical qubit gate, the σ_L^x rotation, requires collective operation on both physical qubits, since $\sigma_L^x \equiv \sigma_P^x \otimes \sigma_P^x$. To realize this operation, a focused beam is centered between a pair of ions, equally illuminating both with a bichromatic light field as described by Mølmer and Sørensen [17]. The two frequencies are $\omega_0 \pm (\omega_z + \delta_{\text{MS}})$, where ω_0 is the transition frequency from $|S\rangle$ to $|D\rangle$, ω_z represents the frequency of the center-of-mass mode in the axial direction ($\omega_z \approx (2\pi)$ 1.2 MHz) and δ_{MS} is a detuning set to (2π) 7 kHz. The light field intensity is chosen such that this operation rotates the corresponding Bloch sphere of the single logical qubit by $\pi/2$ (in the following referred to as $X(\pi/2) \equiv \exp(-i\ \pi/4\ \sigma_L^x)$) after a gate time τ of $\tau(X(\pi/2)) = 2\pi/\delta_{\text{MS}} = 143\mu s$. Our characterization of this operation by measuring the final populations combined with parity oscillations on the output state[20] indicates a fidelity for a logical $\pi/2$ pulse of 96(2)%.

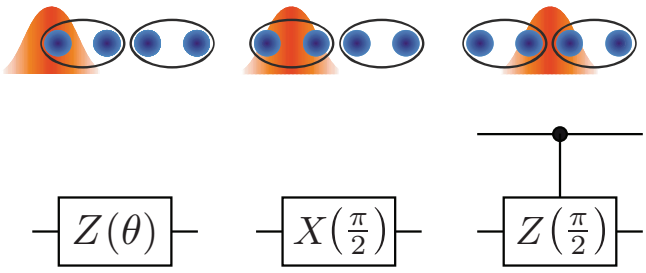

FIG. 1: Set of logical gate operations - σ^z rotation, σ^x rotation and conditional phase gate: A single ion AC-Stark shift pulse allows for arbitrary rotation of the logical qubit around the z-axis; the MS gate represents a rotation about the x-axis of the corresponding Bloch sphere of the logical qubit; the phase gate is realized by a copropagating bichromatic light field as described in [16], applied on adjacent ions of two logical qubits.

The set of universal gates is completed by a two-qubit interaction, here a conditional phase gate. For operations on two logical qubits we work on a string of four ions, where ions 1 and 2 (3 and 4) represent the first (second) logical qubit. Performing a phase gate on the center physical qubits (2 and 3) will translate into a phase gate $\sigma_L^z \otimes \sigma_L^z$ acting on the logical qubits (also see Ref. [19]). For this purpose, the two center ions are illuminated by a bichromatic focused beam realizing a $\sigma_P^z \otimes \sigma_P^z$ gate as proposed in [16]. The frequencies of the bichromatic laser beam are set to $\omega_0 \pm 1/2(\omega_z + \delta_{\text{CP}})$. For our implementation a detuning of about 2 kHz was chosen for δ_{CP}, resulting in a gate time of $\tau(CP) = 2\pi/\delta_{\text{CP}} = 470\mu s$. The performance of this novel phase gate has been investigated by applying it to two ions and carrying out process tomography[21], obtaining a mean gate fidelity of 94(1)%.

We combine single- and two-qubit logical gates to implement the entangling CNOT operation within the chosen DFS. To this end, the logical phase gate is enclosed by two Ramsey pulses on the logical target qubit (see Fig. 2). Depending on the control state the second Ramsey pulse will either flip the target qubit or recover its initial state. Experimentally, we achieve an improved gate fidelity by splitting the phase gate into two pulses, allowing for a spin echo pulse on both logical qubits. The resulting ideal unitary matrix associated with our CNOT

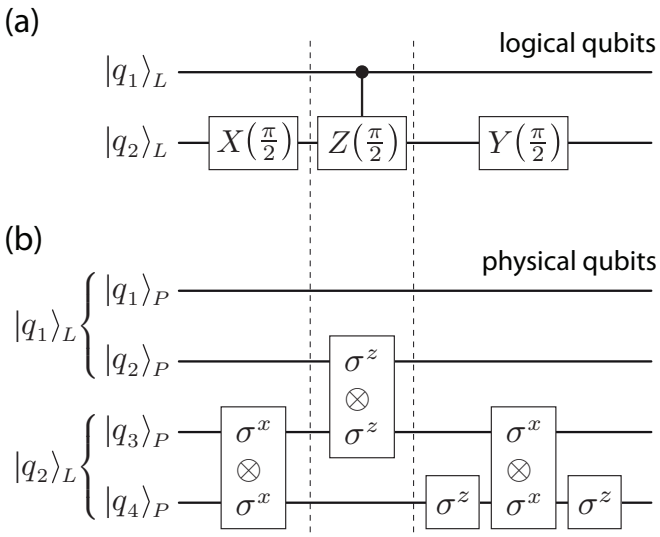

FIG. 2: Pulse sequence to realize a controlled-NOT operation within a DFS - The logical pulse sequence (a) and the operations on the physical qubits (b) are depicted: A logical phase gate is performed on two logical qubits. For the target qubit, the phase gate is enclosed by two Ramsey pulses, respectively $\pi/2$ rotations along the x- and y- axis of the corresponding Bloch sphere (represented by a composite $\sigma^z\sigma^x\sigma^z$ rotation).

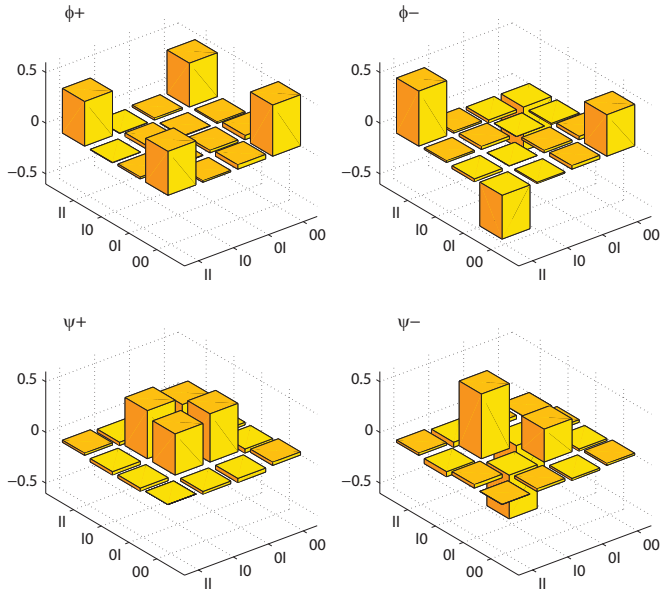

FIG. 3: The DFS-CNOT gate can be used to generate Bell states in the logical qubit Hilbert space. For a given superposition between $|0\rangle_L$ and $|1\rangle_L$ on the control qubit, the resulting output state will be one of the four Bell states. The real part of the obtained density matrices for all four Bell states is shown above. On average, a fidelity of 91(2)% is achieved within the decoherence-free subspace.

operation is:

$$U_{\mathrm{CNOT}} = \begin{pmatrix} 0 & -1 & 0 & 0 \\ i & 0 & 0 & 0 \\ 0 & 0 & 1 & 0 \\ 0 & 0 & 0 & i \end{pmatrix}$$

In order to prove that the gate acts as intended, this CNOT gate is applied to generate entangled states within the DFS. After preparation of one of the four basis states $\{|00\rangle_L, |01\rangle_L, |10\rangle_L, |11\rangle_L\}$, a superposition between the logical ground and excited state of the control qubit is generated by a $X(\pi/2)$ rotation. Subsequent application of the CNOT gate directly maps the input states onto the Bell basis states $\{|\phi^+\rangle_L, |\phi^-\rangle_L, |\psi^+\rangle_L, |\psi^-\rangle_L\}$ defined by $|\phi^\pm\rangle_L = |00\rangle_L \pm |11\rangle_L$ and $|\psi^\pm\rangle_L = |01\rangle_L \pm |10\rangle_L$. In the physical basis, these states are equivalent to four-qubit Schrödinger cat states. The output state is determined by quantum state tomography in the Hilbert space of the four physical qubits. Restricting quantum computation to a subspace of the total Hilbert space leads to two basic questions at the end of a computation: a) Is the outcome within the subspace? b) How close is the result to the expected one? Accepting only results within the DFS allows for computation at higher fidelities, but making it probabilistic. The probability of a state to remain in the DFS after application of a certain gate sequence will be called permanence P. The fidelity of the generated state within the DFS can be calculated in a straightforward manner. The four Bell basis states are obtained with fidelities F of {89(1),91(1),91(1),92(1)}% and a permanence P of {90.2,94.3,83.9,86.0}%. The real part of the obtained density matrices of the four different Bell states are depicted in Fig. 3.

In order to fully characterize the logical CNOT gate, its performance is analyzed by quantum process tomography [21]. For the given two-logical qubit Hilbert space it is performed by creating $4^2 = 16$ linear independent logical input states, applying the CNOT gate, and fully characterizing the output state via state tomography in the physical basis (3^4 settings each). Each experimental setting was repeatedly measured 100 times and averaged, resulting in a total measurement time per setting of about 5 seconds. In total the characterization of the CNOT gate requires about 2 hours of measurement time. Evaluation of this data allows us to derive the so-called χ-matrix that describes the investigated process $\mathcal{E}$, here the CNOT within a DFS, such that $\rho_{out} = \mathcal{E}(\rho_{in}) = \sum_{m,n=1}^{4^N} \chi_{m,n} A_m \rho_{in} A_n^\dagger$, where N is the number of logical qubits, ρ_{in} and ρ_{out} are the input and output density matrices and A is a basis of operators in the Hilbert space of dimension $2^N \times 2^N$ [22]. Taking 2×10^5 pure logical input states, randomly drawn from the unitary group $U(4)$ according to the Haar measure [23], the mean gate fidelity is then calculated by $\bar{F} = \mathrm{mean}_{\psi_i} \left[\langle\psi_i|U^\dagger\ \mathcal{E}(|\psi_i\rangle\langle\psi_i|)\ U|\psi_i\rangle\right]$, where U repre-

sents the ideal unitary map for the implemented process. We infer a mean permanence of the CNOT operation of $\bar{P} = 89(7)\%$ and a mean gate fidelity of $\bar{F} = 89(4)\%$ within the DFS. The overall fidelity of $\bar{P} \cdot \bar{F} \approx 79(7)\%$ is consistent with the achieved fidelities of its constituent operations of about 83(3)%. The mean gate fidelity within the DFS of 89(4)% is comparable with current state-of-the-art two-qubit quantum gates acting on selected qubits out of a quantum register, operating at a fidelity of 92.6(6)% [21].

Infidelities of the gate can be classified according to their effect on the permanence or gate fidelity within the DFS. Addressing errors constitute the main error source for leaving the DFS during a pulse sequence. When focusing the laser down onto a pair of two ions, some residual light is also applied to the adjacent ions. The addressing error is characterized by the ratio of the Rabi frequency of a logical qubit compared to the Rabi frequency of an adjacent, single ion. For the chosen parameters the ratio was about 5%. This unwanted excitation on the neighboring ion results in a population loss from the DFS. Another error source for leaving the DFS are off-resonant excitations during the bichromatic gates. To minimize this error we use amplitude-shaped laser pulses as described in [24]. Errors within the DFS are mainly due to unbalanced intensities of the light fields acting on the two simultaneously addressed ions. The difference between the Rabi frequencies is caused by beam pointing instability with regard to the ion position. Finally, intensity fluctuations lead directly to phase errors of the single-logical qubit phase gate via the intensity dependence of the AC-Stark effect. Note that laser frequency and magnetic field fluctuations do not contribute to errors since the DFS encoding protects against such decoherence. All shortcomings described above are caused by technical imperfections and do not represent a fundamental limit to the achievable fidelities. Spontaneous decay of the excited level as the only fundamental error can be avoided by encoding the physical qubits in the two Zeeman-ground states.

To conclude, we have demonstrated a universal set of quantum gates acting in a decoherence-free subspace of trapped ions, consisting of addressable gate operations, namely: single logical qubit σ_L^z and σ_L^x as well as a two logical qubit phase gate $\sigma_L^z \otimes \sigma_L^z$. Using these gates we have implemented and characterized a controlled-NOT gate within a decoherence free subspace acting on logical ion qubits. Our implementation achieves fidelities close to current state-of-the-art quantum computation as well as it employs logical qubits with a coherence time one hundred times longer than their single constituents.

We gratefully acknowledge support by the Austrian Science Fund (FWF), by the European Commission (SCALA), and by the Institut für Quanteninformation GmbH. This material is based upon work supported in part by IARPA. T.M. and K.K. contributed equally to this work.

* Current Address: Department of Physics and Joint Quantum Institute, University of Maryland, College Park, Maryland, 20742, USA
† Current Address: Institute of Optics, Information and Photonics, University of Erlangen-Nürnberg, Staudtstrasse 7/B2, 91058 Erlangen, Germany
‡ Current Address: Department of Physics, University of California, Berkeley, 366 LeConte Hall #7300, CA 94720-7300, USA

[1] A. Steane, Proc. Roy. Soc. A **452**, 2551 (1996).
[2] A. R. Calderbank and P. W. Shor, Phys. Rev. A **54**, 1098 (1996).
[3] J. Chiaverini, et al., Nature **432**, 602 (2004).
[4] D. A. Lidar, I. L. Chuang, and K. B. Whaley, Phys. Rev. Lett. **81**, 2594 (1998).
[5] P. Kwiat, et al., Science **290**, 498 (2000).
[6] M. Bourennane, et al., Phys. Rev. Lett. **92**, 107901 (2004).
[7] L. Viola, et al., Science **293**, 2059 (2001).
[8] C. F. Roos, et al., Phys. Rev. Lett. **92**, 220402 (2004).
[9] H. Häffner, et al., et al., Appl. Phys. B **81**, 151 (2005).
[10] D. Kielpinski, et al., Science **291**, 1013 (2001).
[11] J. E. Ollerenshaw, D. A. Lidar, and L. E. Kay, Phys. Rev. Lett. **91**, 217904 (2003).
[12] D. Kielpinski, C. Monroe, and D. J. Wineland, Nature **417**, 709 (2002).
[13] T. Sleator and H. Weinfurter, Phys. Rev. Lett. **74**, 4087 (1995).
[14] D. P. DiVincenzo, Phys. Rev. A **51**, 1015 (1995).
[15] F. Schmidt-Kaler, et al., Appl. Phys. B **77**, 789 (2003).
[16] K. Kim, et al., Phys. Rev. A **77**, 050303(R) (2008).
[17] A. Sørensen and K. Mølmer, Phys. Rev. Lett. **82**, 1971 (1999).
[18] P. Lee, et al., J. Opt. B **7**, S371 (2005).
[19] L. Aolita, et al., Phys. Rev. A **75**, 052337 (2007).
[20] D. Leibfried, et al., Nature **422**, 412 (2003).
[21] M. Riebe, et al., Phys. Rev. Lett. **97**, 220407 (2006).
[22] I. Chuang and M. Nielsen, J. Mod. Opt. **44**, 2455 (1997).
[23] M. Pozniak, K. Zyczkowski, and M. Kus, J. Phys. A: Math. Gen. **31**, 1059 (1998).
[24] C. F. Roos, New J. Phys. **10**, 013002 (2008).